Supplementary Information (SI) for Journal of Materials Chemistry C.

Artificial light harvesting gel based on saponification triggered gelation of aggregation induced emissive BODIHYs

Durgendra Yadav[a], Vishwa Deepak Singh[b], Ashish Kumar Kushwaha[a], Anjani Kumar[a], Roop Shikha Singh[a*]

[a]Department of Chemistry, Institute of Science, Banaras Hindu University, Varanasi– 221 005 (U. P.) India

[b]Department of Chemistry, D.A.V. P.G. College, Gorakhpur – 273001 (U. P.) India

Experimental

Materials

4–aminobenzoic acid, 5–aminoisophthalic acid, N,N-diisopropyl–ethylamine, and borontrifluoride etherate were purchased from Sigma Aldrich India. Common reagents, sodium acetate, NaOH, C_2H_5OH, HCl, $NaNO_2$ and the solvents ethyl acetate, hexane, dimethylsulphoxide (DMSO), dichloromethane (DCM), dimethylformamide (DMF) and methanol etc. were procured from Avra Chemicals Hyderabad, India and dried and distilled following standard literature procedures.[1] The synthetic manipulations have been performed under oxygen free nitrogen atmosphere and photophysical studies made using spectroscopic grade solvents.

General information

^{1}H (500 MHz), ^{13}C (125 MHz), ^{11}B (160 MHz) and ^{19}F (470 MHz) NMR spectra have been obtained on a JEOL AL 500 FT–NMR spectrometer at room temperature using $Si(CH_3)_4$ as an internal whereas $BF_3{\cdot}OEt_2$ and CF_3COOH as external reference. UV–vis and emission spectra have been acquired at room temperature on a Shimadzu UV–1800 and Perkin Elmer LS55 Fluorescence spectrometers. Electrospray ionization Mass Spectrometric (ESI–MS) measurements have been made on a Bruker–Daltonics mass spectrometer. Time resolved fluorescence lifetime experiments have been made on a TCSPC system from Horiba Yovin (Delta Flex). Compounds were excited at 368 nm using a pico–second diode laser (Model: Delta Diode). Data analysis has been performed using decay analysis software (HORIBA Scientific: EzTime). Scanning electron microscopic images were captured on quanta 200 F microscope using silicon wafer. Dynamic light scattering (DLS) studies were performed on a ZetaSizer Ultra (ZSU5700) instrument from Malvern Panalytical, Atomic force microscope (AFM) images were captured on a NTMDT Solver NEXT Russia, Transmission electron microscope (TEM) was carried out using TECHNAI G^2 20 TWIN, FE, USA, Rheological studies were done by Anton-Paar MCR 72 rheometer and MCR 102 (Anton Paar).

Preparation of gel (GL_2 and GB_2)[8]: Stock solution of **L2** and **B2** (*c*, 1.0×10^{-2} M in $CHCl_3$) and NaOH (*c*, 2.0 M in MeOH) were prepared and filtered to obtain a clear solution. For gelation a solution of NaOH (2.0 equiv) was added to a freshly prepared solution of **L2** and **B2** (1.0 mL) with 1 or 2 strokes of shaking. Almost instantaneously (within a minute) it gave a gel material (**GL_2** and **GB_2**).

AFM, SEM and TEM: Diluted gels (~10^{-4} M) were used for AFM whereas vacuum dried gels were used for SEM analysis. Samples were prepared by smearing a small amount of freshly prepared gels on a carbon-coated Cu TEM grid (300 mesh), which was air-dried at room temperature before imaging at an accelerating voltage of 200 kV without staining.

Rheology Experiments: Viscoelastic nature of the gels $\mathbf{G_{L2}}$ and $\mathbf{GB_2}$ were studied individually by dynamic rheology, where viscous (storage, G′) and elastic (loss, G″) moduli were plotted against oscillatory strain (γ, %) and angular frequency (ω, rad/s). Dynamic oscillatory work kept at a frequency of 1 to 10 rad/s. A small amount of freshly prepared gel was scooped out and placed on the stationary plate of the rheometer, and parallel-plate geometry (20 mm diameter, 0.2 mm gap) was employed to perform the rheological experiments.

Single crystal analysis[2-4]**:** Single crystal X–ray data has been collected on a Bruker APEX–II CCD diffractometer at 293 K (**L1**, **L2**, **B1** and **B2**) equipped with a Mo–Kα (λ = 1.54184 Å, graphite monochromator) radiation. The φ and ω scan modes were employed for data collection. Structures have been refined by direct methods (SHELXS 97) followed by full–matrix least squares on F^2 (SHELX 14) within the OLEX^2 environment. All the atoms (except H) were assigned anisotropically. Interaction and stacking distances were analyzed using PLATON. Files related to crystal data have been submitted with CCDC deposition numbers are 2337969 (**L1**), 2337970 (**L2**), 2309327 (**B1**) and 2309328 (**B2**). Crystallographic data and refinement parameters for hydrazone ligands and BODIHYs are summarized in Tables S1–S3. We obtained single crystals of ligands and BODIHYs by slow evaporation of CH_2Cl_2/CH_3OH solution over a period of three weeks.

Theoretical studies[5-7]**:** The geometry optimizations for ligands, BODIHYs and their saponified gels have been made by density function theory (DFT) using GAUSSIAN 09 program package at B3LYP levels. Geometry for ligands and BODIHYs has been taken from single crystal X–ray data for optimization. The 6–31G** basis set has been used for non–metal atoms (C, H, N, S, O, B, F) for geometry optimization and conformational stability in gaseous state. The time–dependent DFT (TD–DFT) has been performed for investigating UV–vis spectra of the ligands and BODIHYs using same basis sets.

UV/vis and Fluorescence Titration Study: Stock solutions of **L2** and **B2** (10 mM) in $CHCl_3$ and NaOH (0.1 M) in CH_3OH were prepared. Concentration of **L2** and **B2** were optimized

and fixed close to the gelation concentration as much as possible within instrument limits to observe genuine changes of added NaOH. In a typical UV/vis experiment, solution of these were taken in 3 mL quartz cuvettes in which, measured quantity of NaOH was added with the help of a micropipette. Further for fluorescence titration studies stock solutions of **L2** and **B2** in $CHCl_3$ (10 mM) and NaOH (0.1 M) in methanol were prepared. Fluorescence spectra of the complexes recorded at gelation concentration to find out changes during gelation as much as close to certainty on the experimental ground.

Energy Transfer and Antenna Effect Calculations: ALHSs study has been mentioned only for BODIHYs complexes and prolific results for ligands may not obtained. It is because of very less overlapping between the emission spectra of ligands with absorption spectra of RhB.

Further, to calculate the light harvesting ability of the system energy transfer efficiency was calculated from excitation spectra using equation 1.

$$\phi_{ET} = 1 - I_{DA}/I_D \quad .....(1)$$

where I_D and I_{DA} are the fluorescence intensity of the excitation of **B1**/**RhB**, **B2**/**RhB** and **GB_2**/**RhB** (donor and acceptor) and **B1**, **B2** and **GB_2** (donor) at 428, 421 and 430 nm, respectively.

The energy-transfer efficiency (Φ_{ET}) was calculated as 58%, 3.4% (in f_w 90%) and 26% (in chloroform), measured under the condition of [**B1**], [**B2**] and [**GB_2**] = 5×10^{-5} M, [RhB] = 1.8×10^{-6} M and λ_{ex} = 428, 421 and 430 nm, respectively.

The antenna effect (AE) was calculated based on the excitation spectra using equation 2.

$$I_a = (I_{A+D(\lambda ex)} - I_{D(\lambda ex)}) / I_{A+D(\lambda ex\,=\,540nm)} .....(2)$$

where I_{A+D} (λ_{ex}) and I_{A+D} (λ_{ex} = 540 nm) are fluorescence intensities at 583, 585 and 577 nm with excitation of the donor at 428 (**B1**), 421 (**B2**) and 430 (**GB_2**) nm and direct excitation of the acceptor at 540 nm, respectively.

The antenna effect was calculated as 16.4, 15.6 (in f_w 90%) and 4.4 (in chloroform), measured under the condition of [**B1**], [**B2**] and [**GB_2**] = 5×10^{-5} M, [RhB] = 1.8×10^{-6} M.

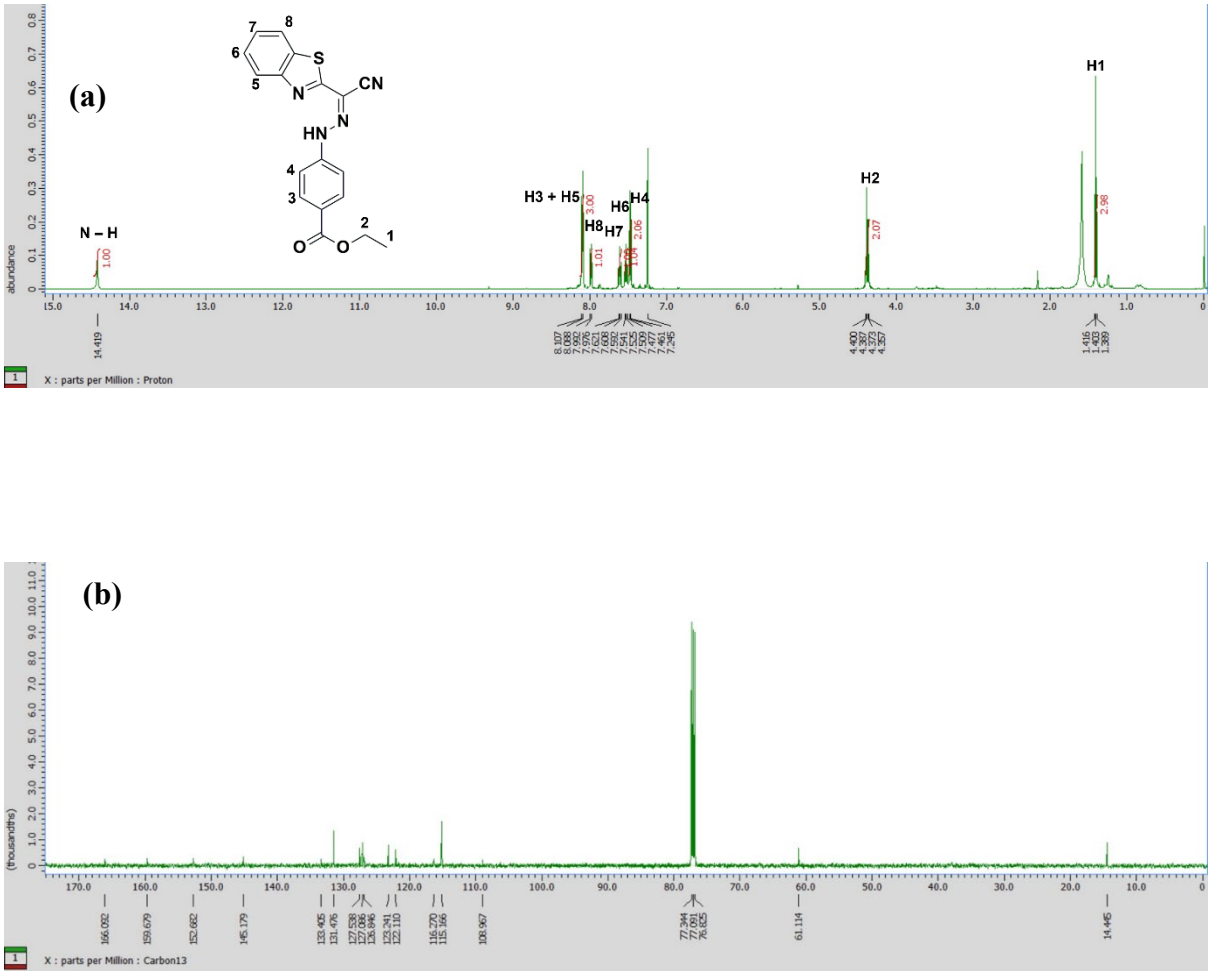

Fig. S1. ^{1}H (a) and ^{13}C (b) NMR spectra of **L1**.

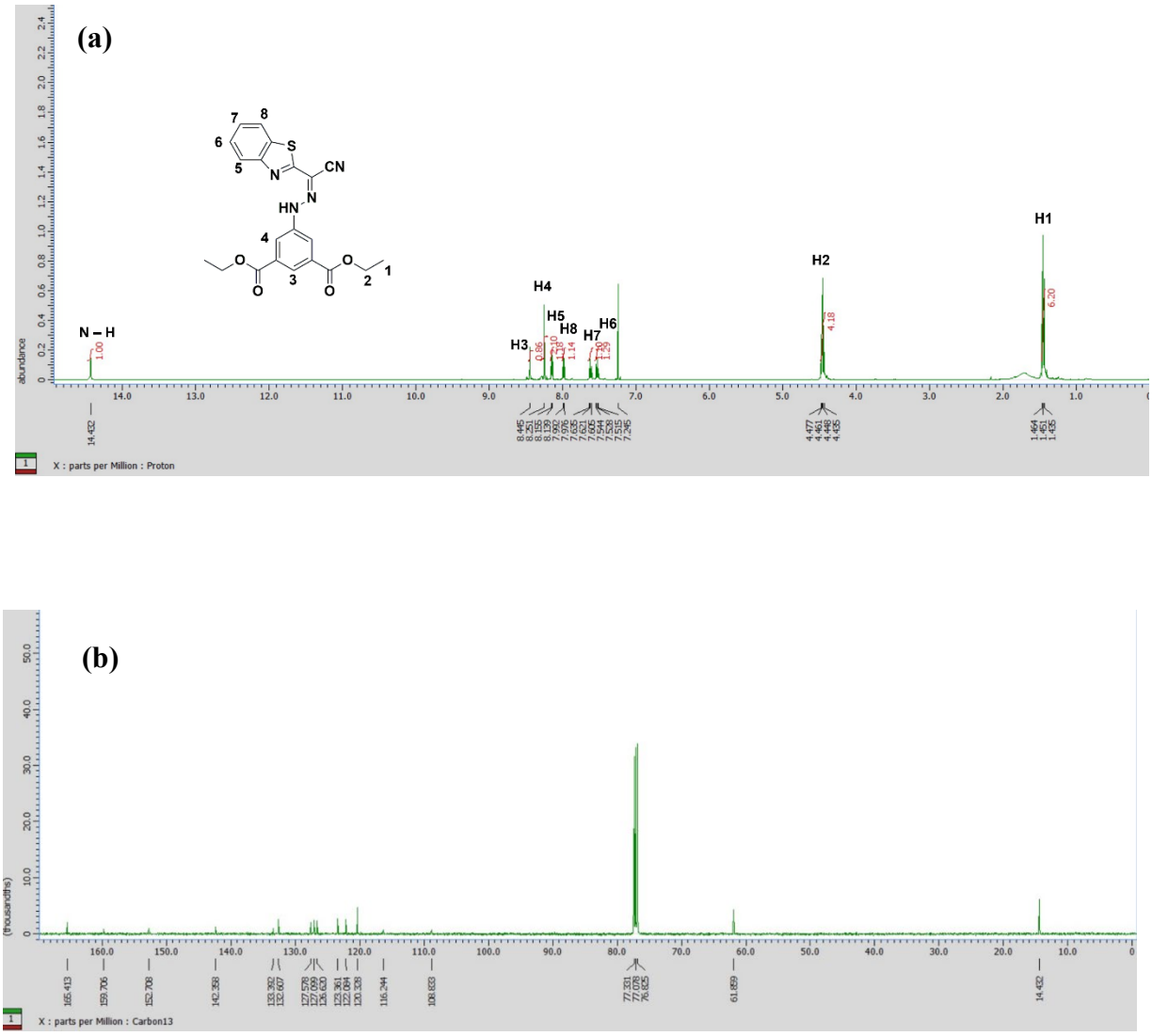

Fig. S2. ^{1}H (a) and ^{13}C (b) NMR spectra of **L2**.

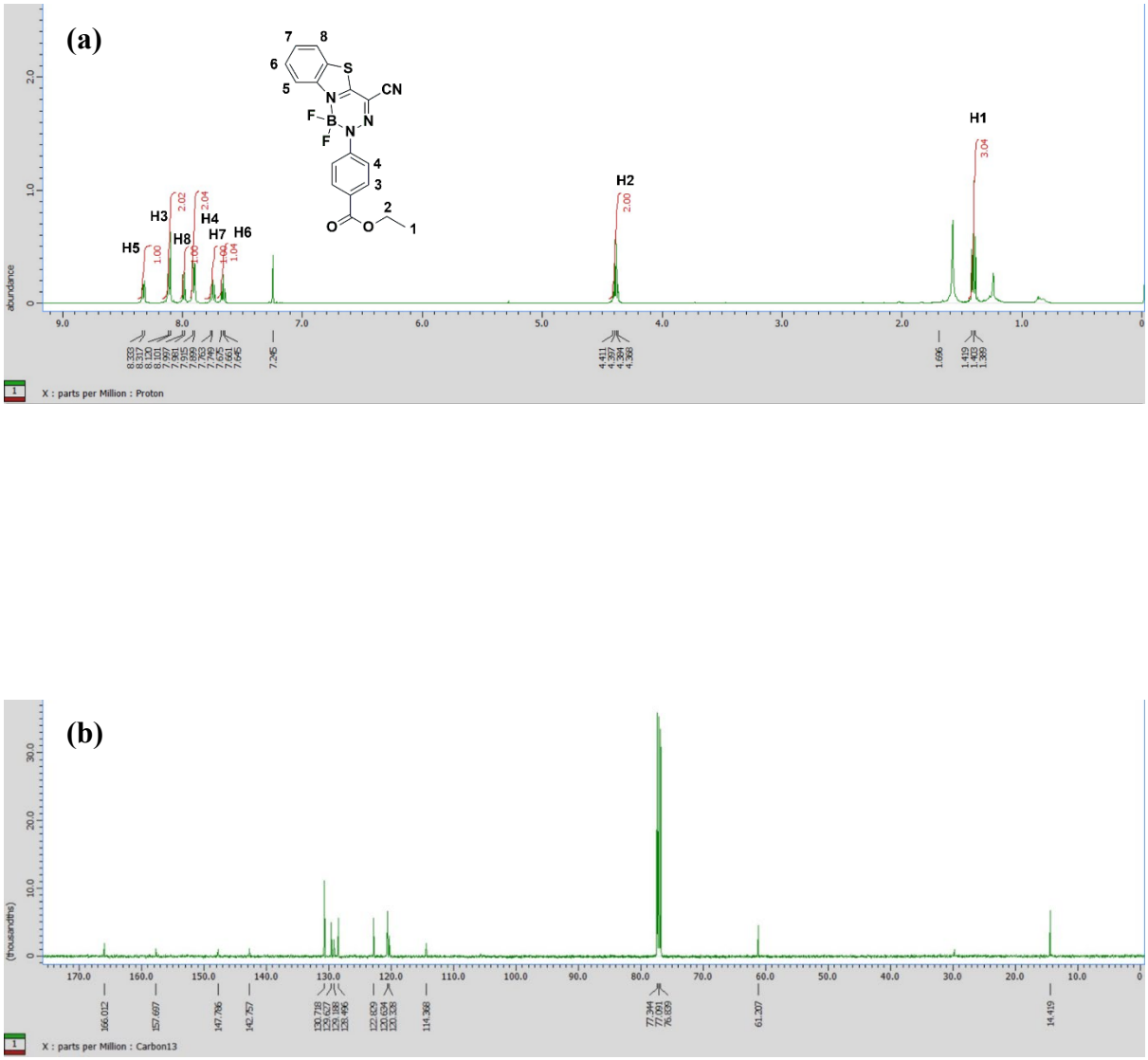

Fig. S3. ^{1}H (a) and ^{13}C (b) NMR spectra of **B1**.

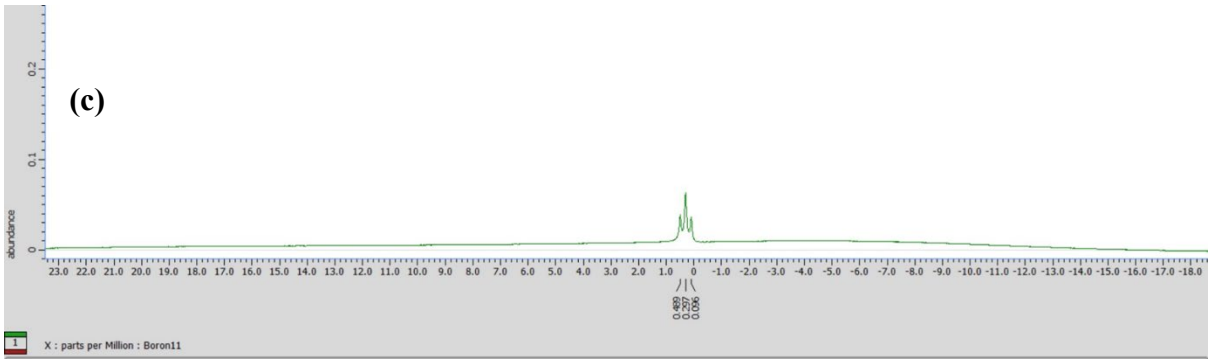

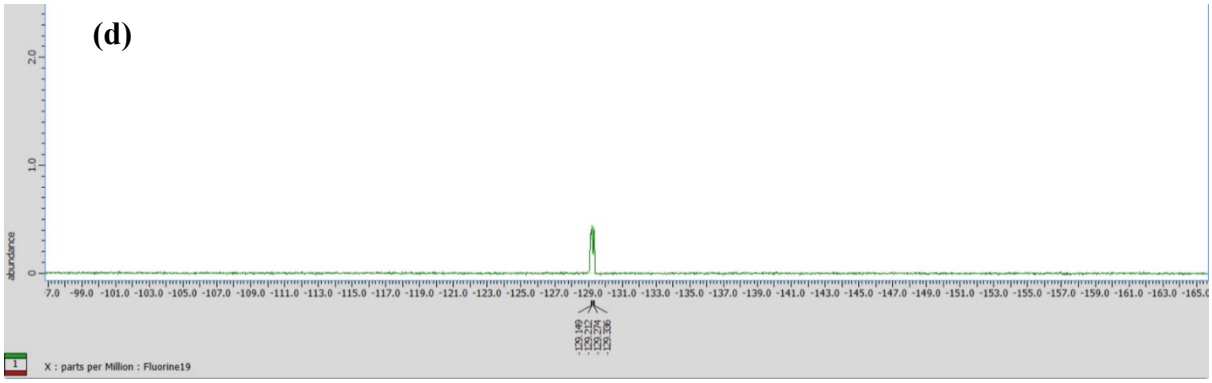

Fig. S4. ^{11}B (c) and ^{19}F (d) NMR spectra of **B1**.

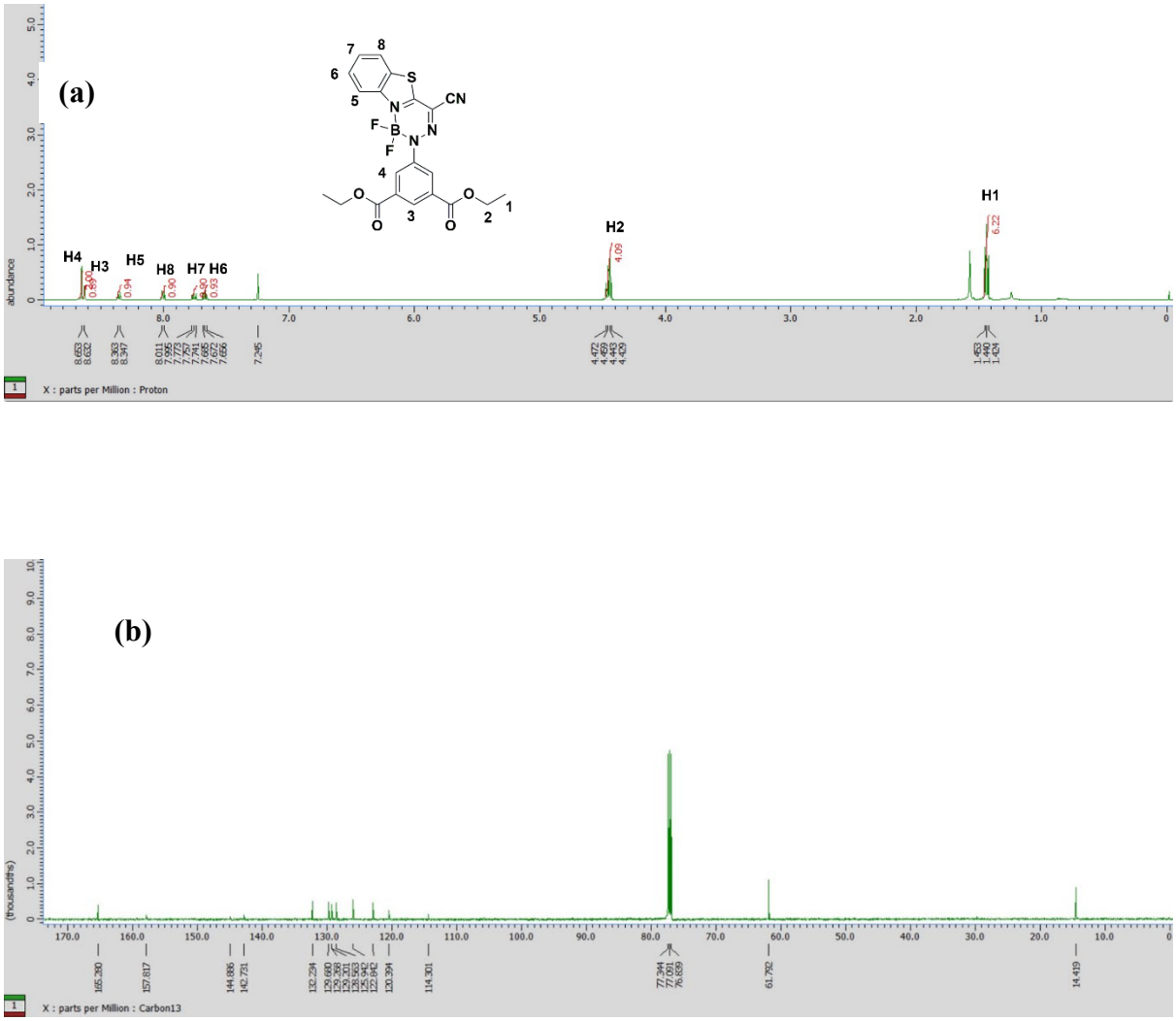

Fig. S5. ^{1}H (a) and ^{13}C (b) NMR spectra of **B2**.

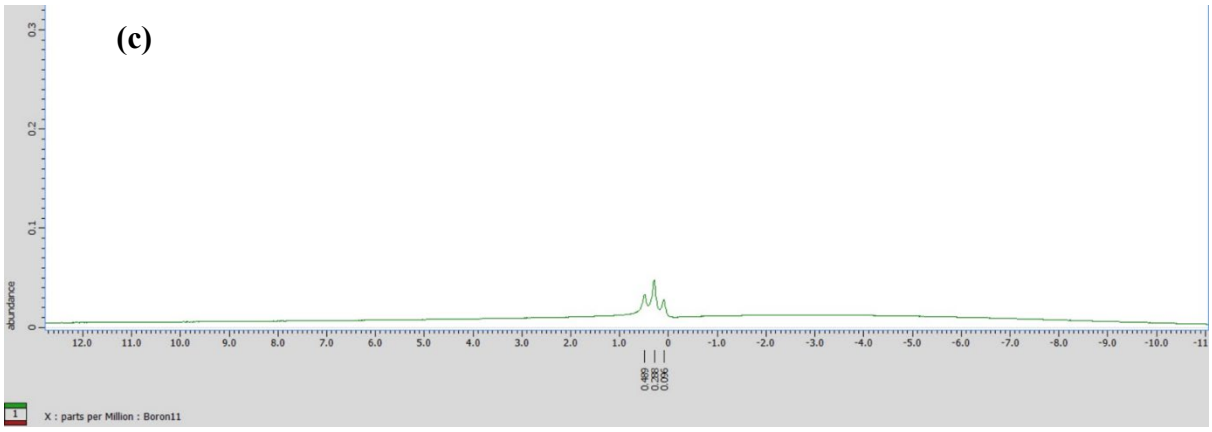

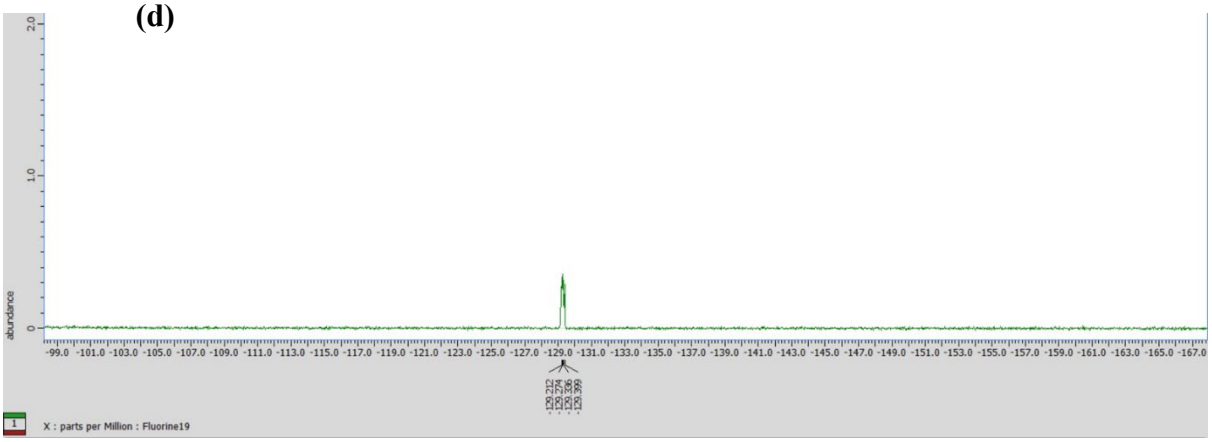

Fig. S6. ^{11}B (c) and ^{19}F (d) NMR spectra of **B2**.

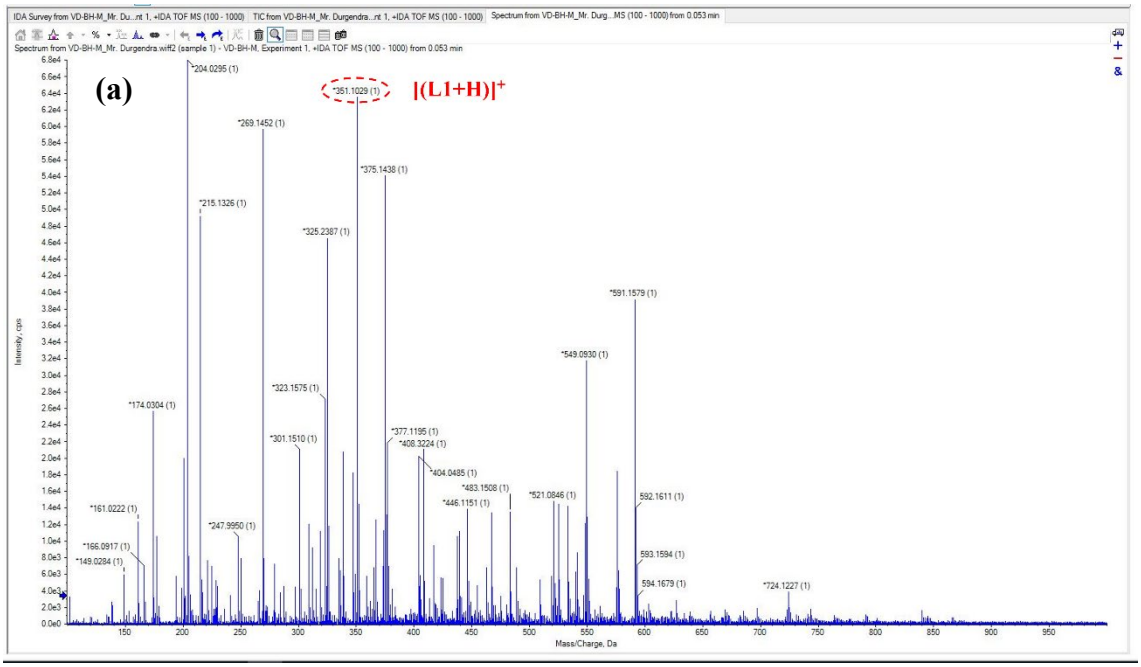

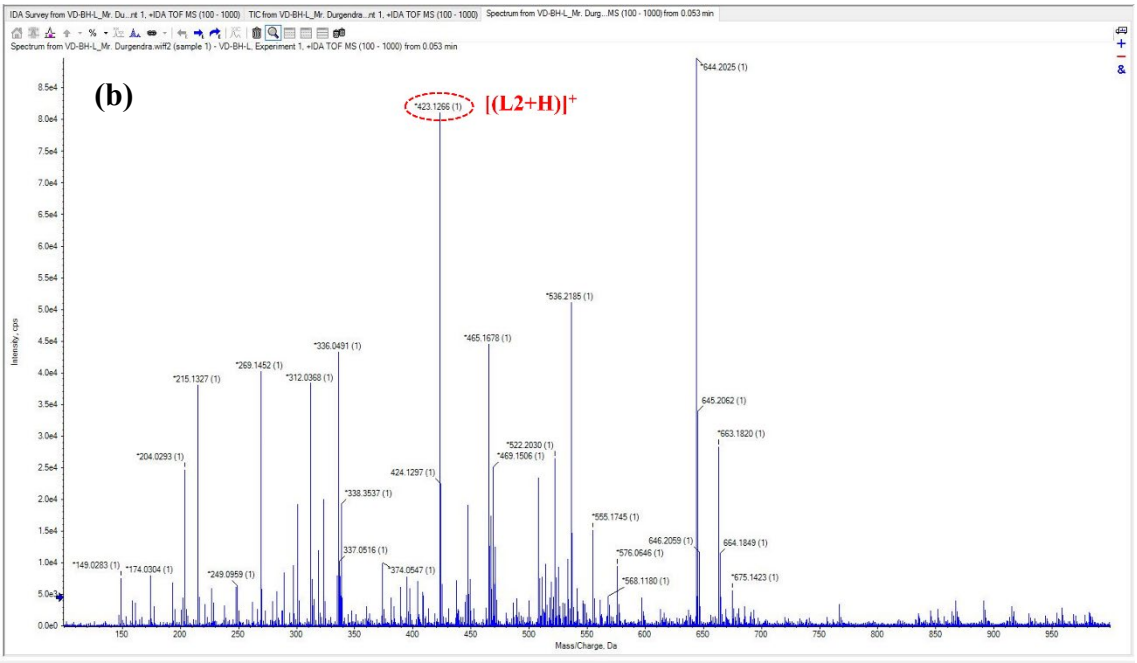

Fig. S7. Mass spectra of **L1** (a) and **L2** (b).

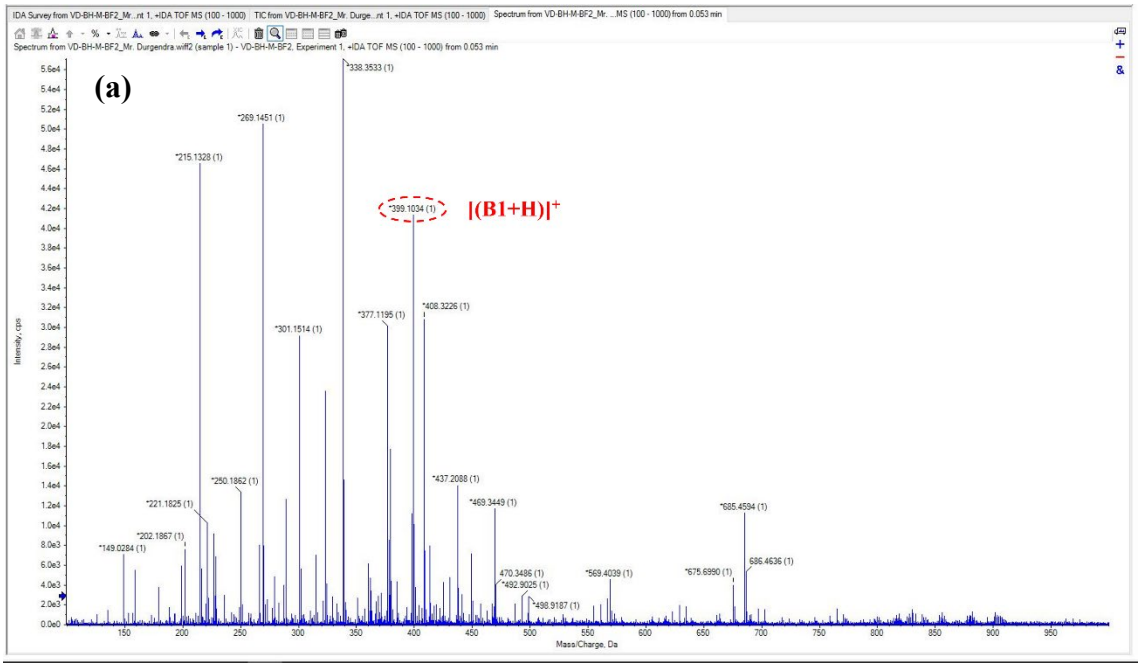

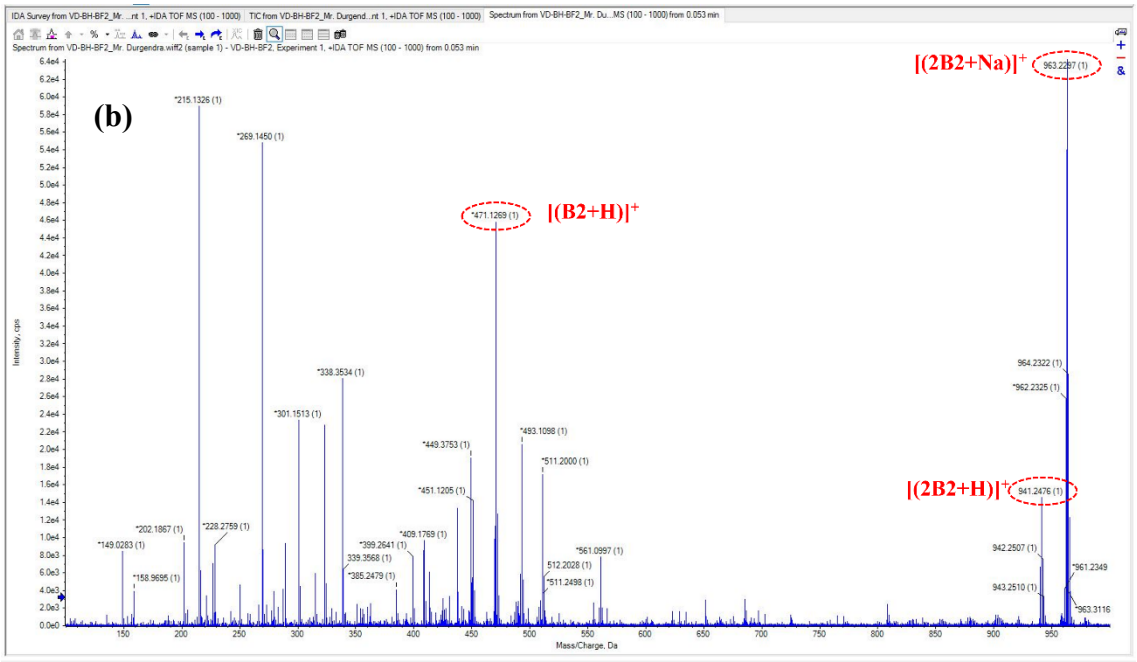

Fig. S8. Mass spectra of **B1** (a) and **B2** (b).

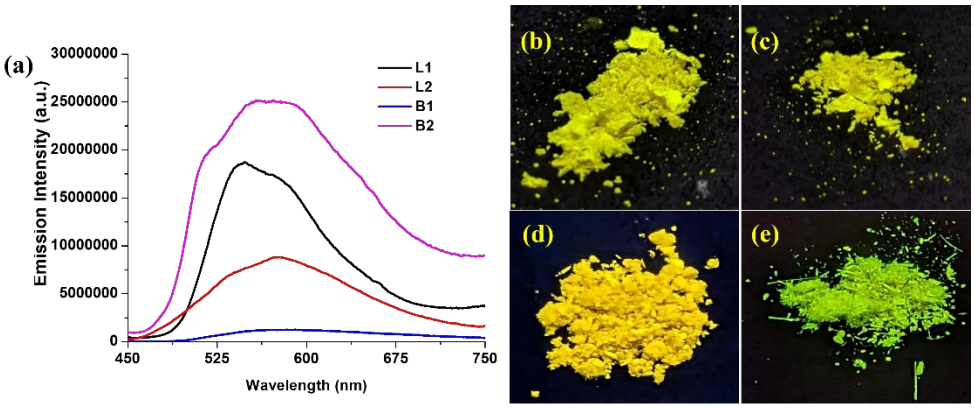

Fig. S9. Solid state emission spectra of **L1**, **L2**, **B1**, **B2** (a), **L1** (b), **L2** (c), **B1** (d), **B2** (e) under the UV radiation of 365 nm.

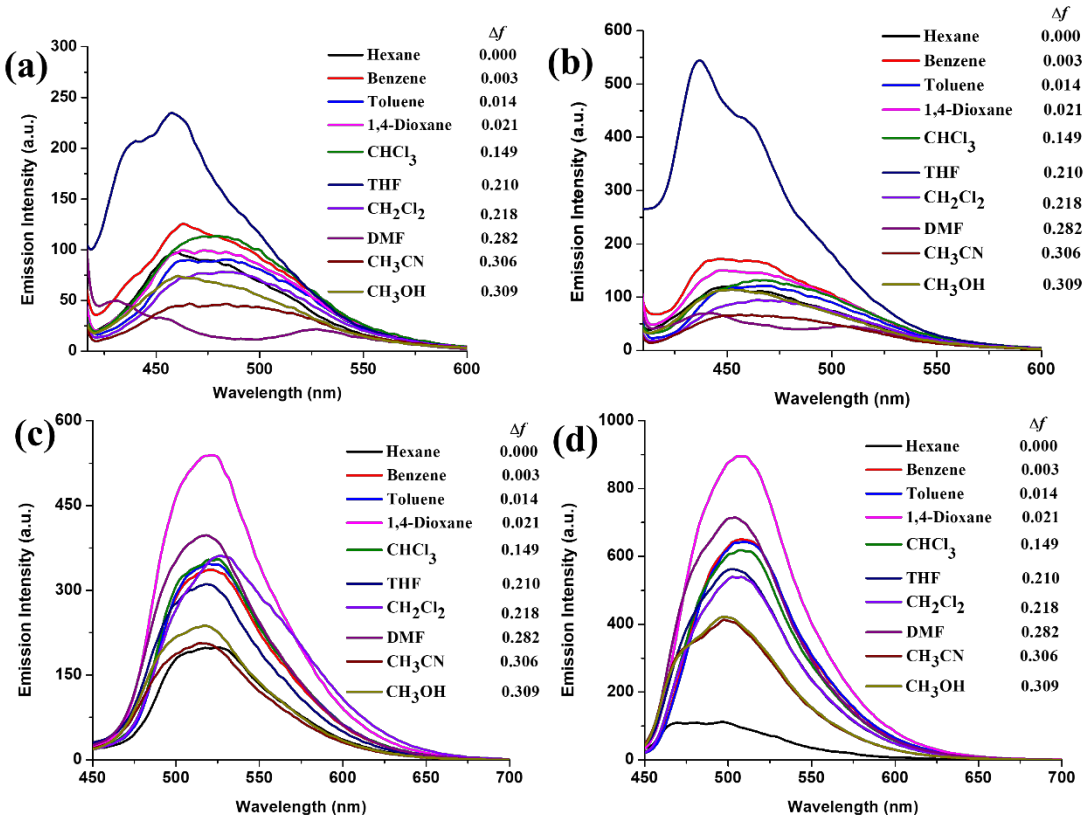

Fig. S10. Emission spectra of **L1** (a), **L2** (b), **B1** (c) and **B2** (d) in various solvent polarities (*c*, 5.0×10^{-5} M).

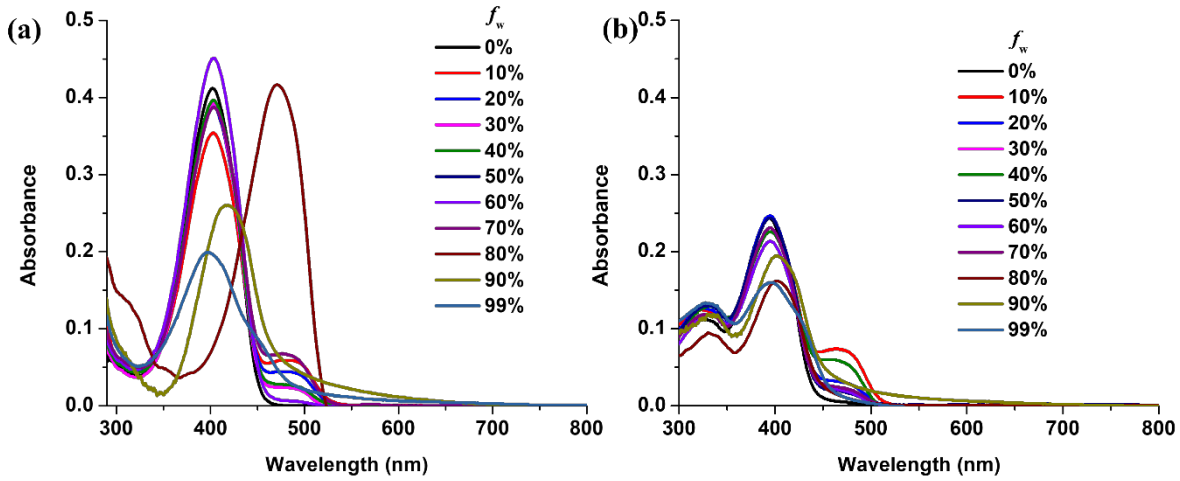

Fig. S11. Absorption spectra of **L1** (a) and **L2** (b) in THF/water fraction (c, 5.0 × 10^{-5} M).

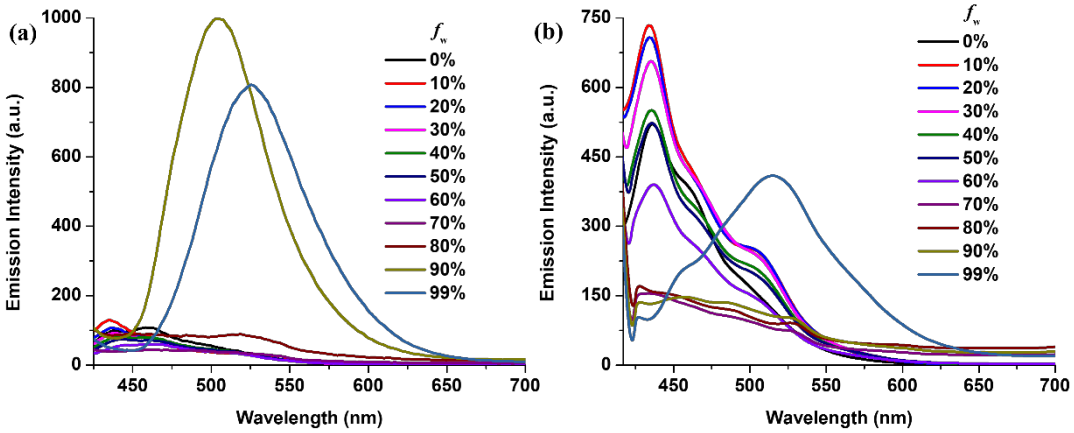

Fig. S12. Emission spectra of **L1** (a) and **L2** (b) in THF/water fraction (c, 5.0 × 10^{-5} M).

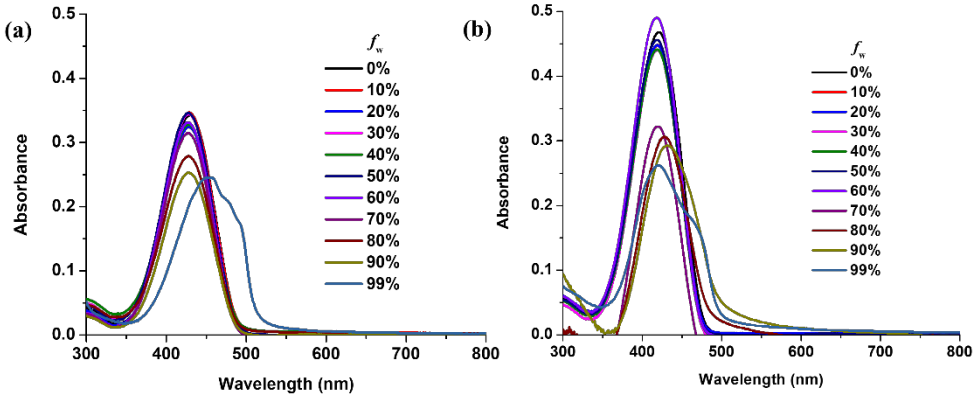

Fig. S13. Absorption spectra of **B1** (a) and **B2** (b) in THF/water fraction (c, 5.0 × 10^{-5} M).

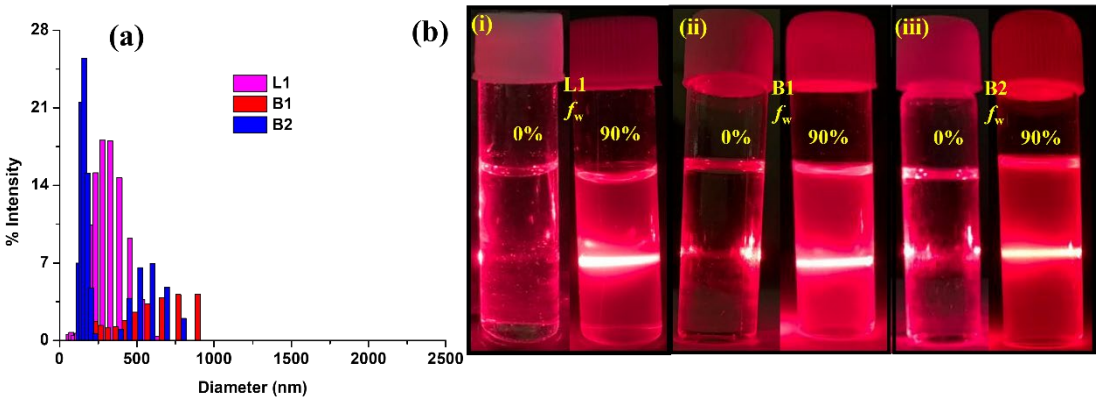

Fig. S14. Dynamic light scattering for **L1**, **B1** and **B2** (a) in the THF/water mixture (f_w = 90%) and images of Tyndall effect in **L1**, **B1** and **B2** (b) in THF and THF/water mixture (f_w = 90%) (c, 5.0 × 10^{-5} M).

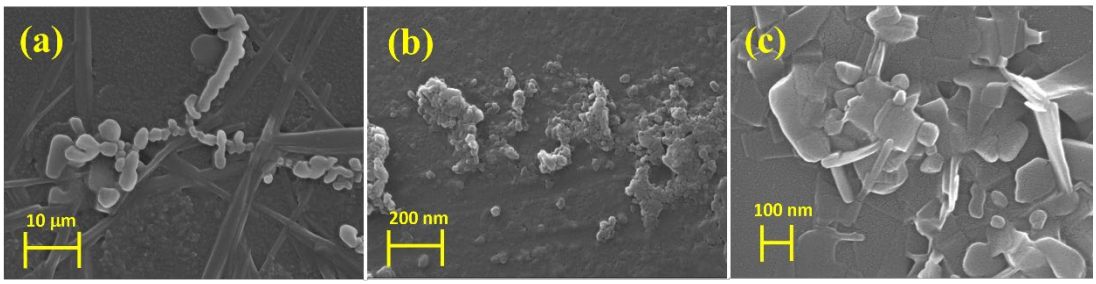

Fig. S15. SEM images of aggregates of **L1** (a), **B1** (b) and **B2** (c) formed in mixture of THF/water (f_w = 90%) (c, 5.0 × 10^{-5} M).

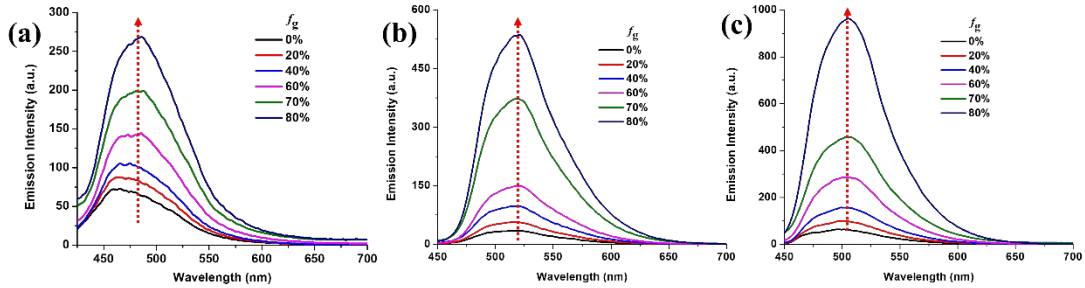

Fig. S16. Emission spectra of **L1** (a), **B1** (b) and **B2** (c) in CH_3OH/glycerol fraction (c, 5.0 × 10^{-5} M).

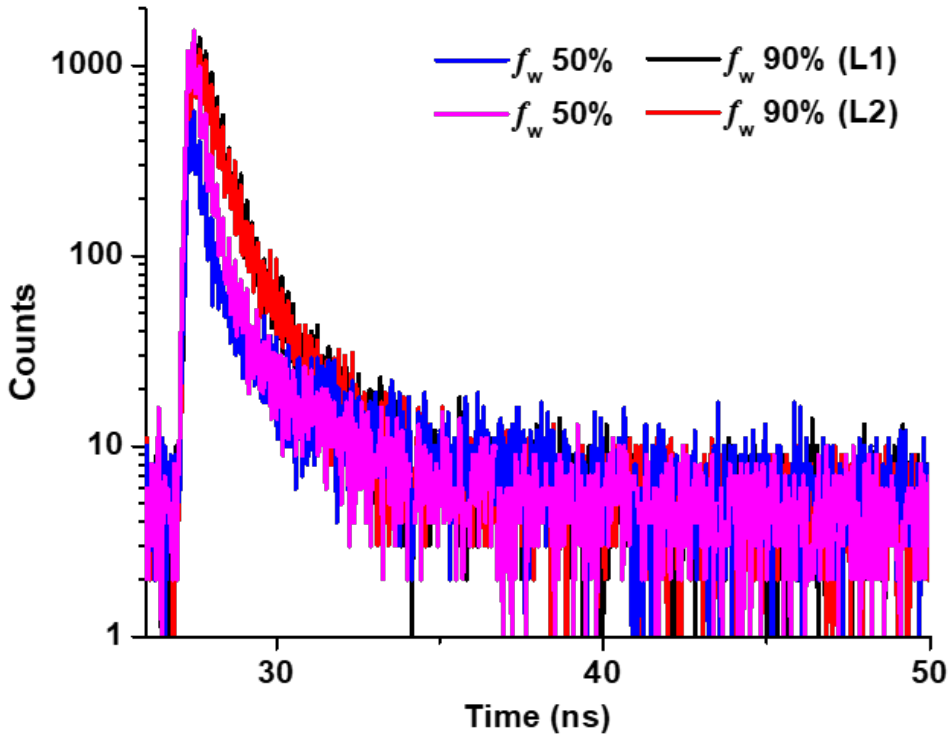

Fig. S17. A logarithmic view of time–resolved fluorescence of **L1** and **L2** in THF (f_w = 50%) and THF/water (f_w = 90%) (c, 5.0 × 10^{-5} M).

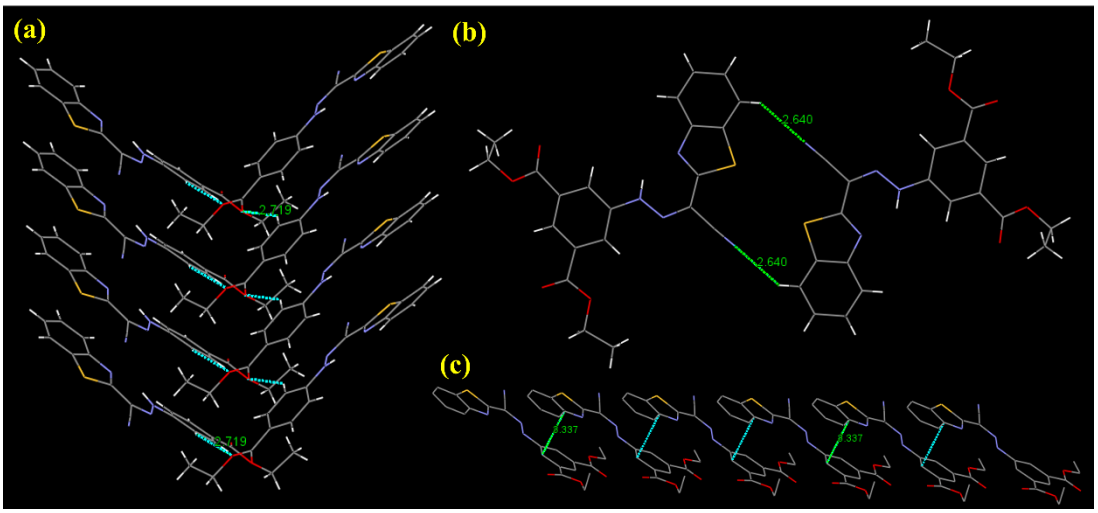

Fig. S18. Crystal packing patterns involving O···H (a) interaction in **L1** and N···H (b) and π···π (c) interactions in **L2**.

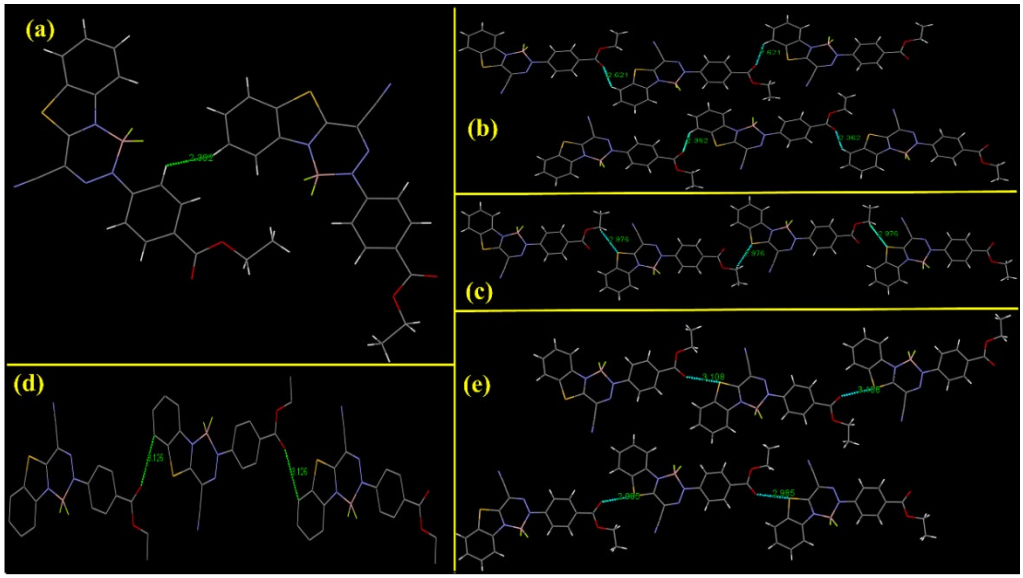

Fig. S19. Crystal packing patterns involving C–H···H–C (a); O···H (b); S···H (c); π···O (d) and S···O (e) interactions in **B1**.

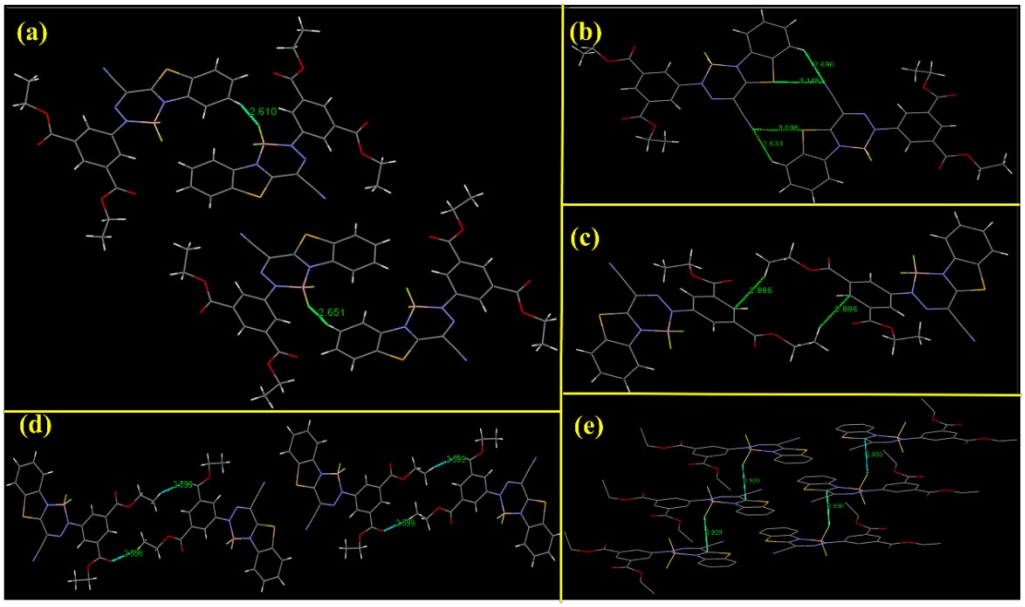

Fig. S20. Crystal Packing patterns through F···H (a); N···H and S···N (b); π···H (c); O···H (d) and π···F (e) interactions in **B2**.

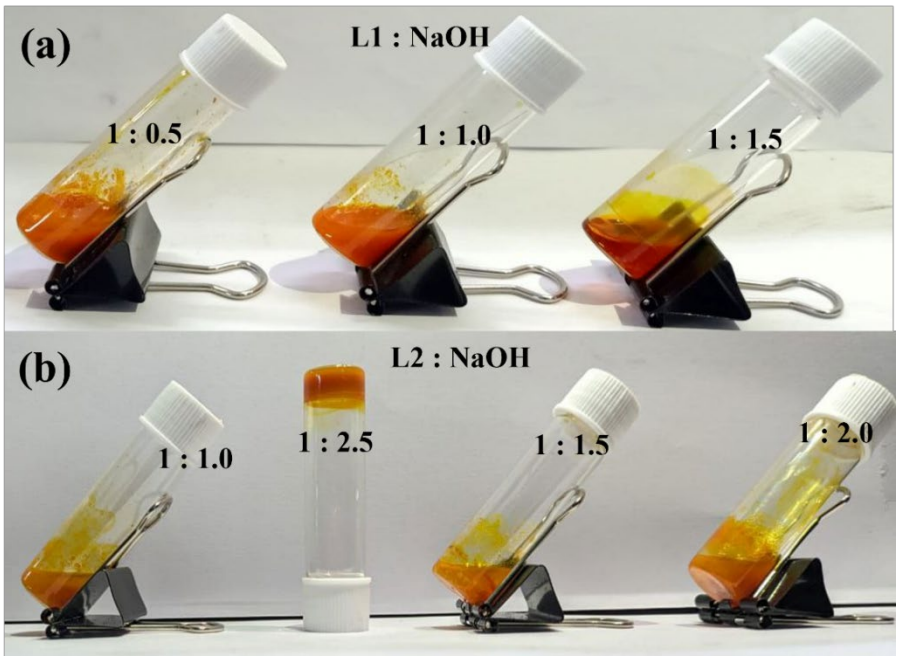

Fig. S21. Photographs of (a) $\mathbf{GL_1}$, (b) $\mathbf{GL_2}$ in inverted vial under naked eye and optimization of stoichiometric ratio of **L2**: NaOH for creating a strong gel (pictures taken after 10 minutes).

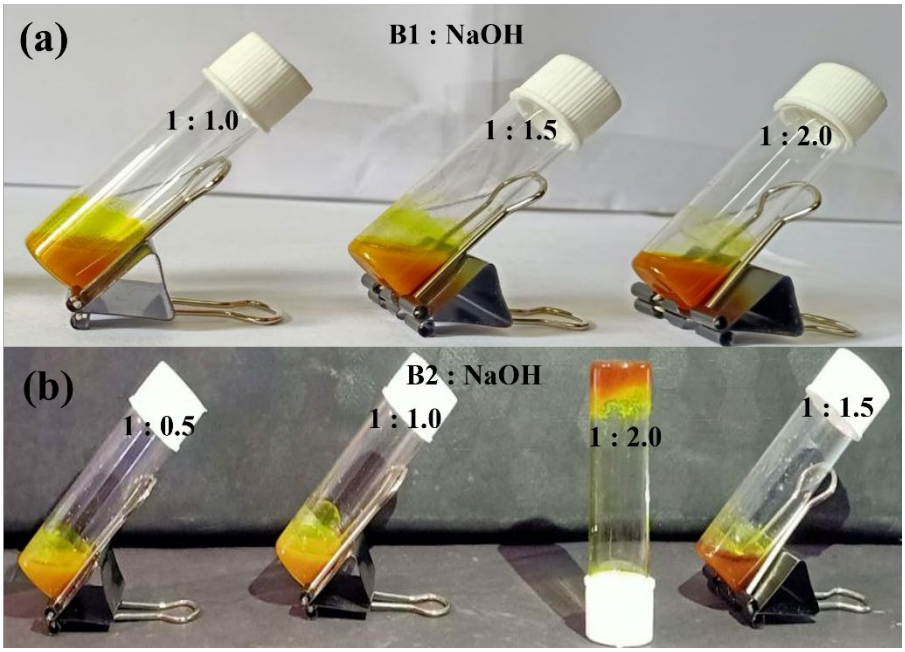

Fig. S22. Photographs of (a) $\mathbf{GB_1}$, (b) $\mathbf{GB_2}$ in inverted vial under naked eye and optimization of stoichiometric ratio of **B2**: NaOH for creating a strong gel (pictures taken after 10 minutes).

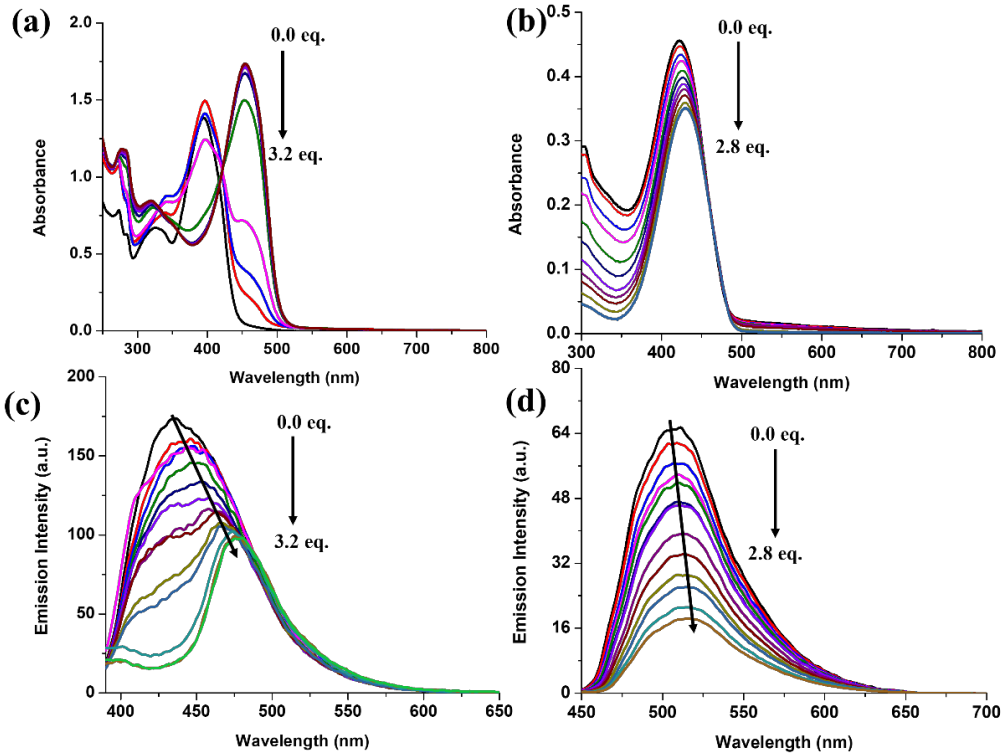

Fig. S23. Absorption (a, **L2**; b, **B2**) and emission spectra (c, **L2**; d, **B2**) in presence of various equivalents of NaOH solution in chloroform.

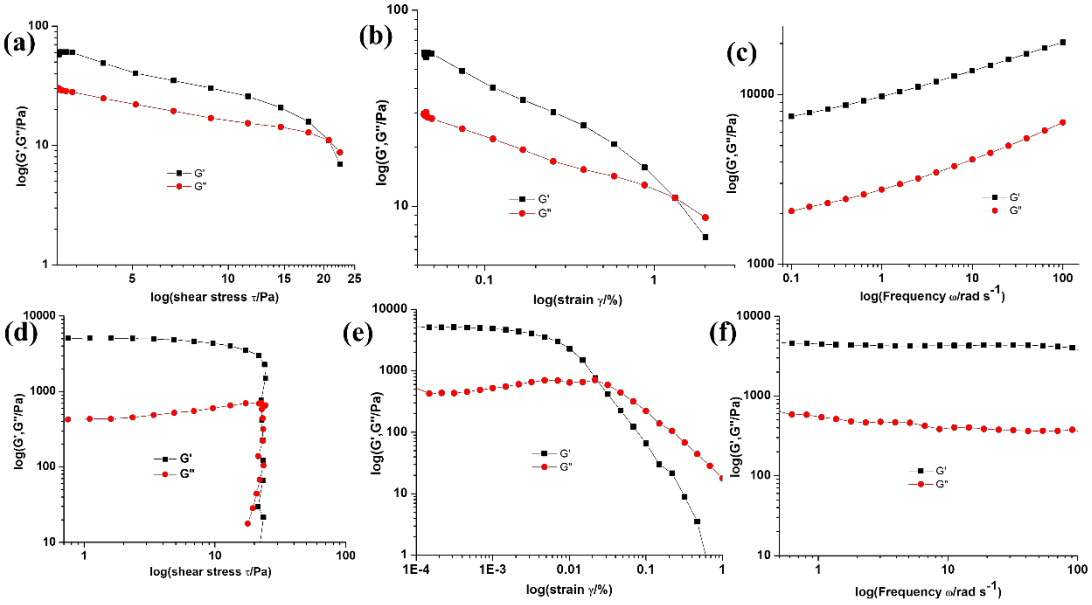

Fig. 24. Dynamic frequency sweep for G′ and G″ for gel **GL₂** (a) and **GB₂** (d) with the applied strain, Dynamic shear stress of G′ and G″ for **GL₂** (b) and **GB₂** (e) at frequency of 1 rad s^{-1} and 25 °C and Dynamic frequency sweep for G′ and G″ for gel **GL₂** (c) and **GB₂** (f).

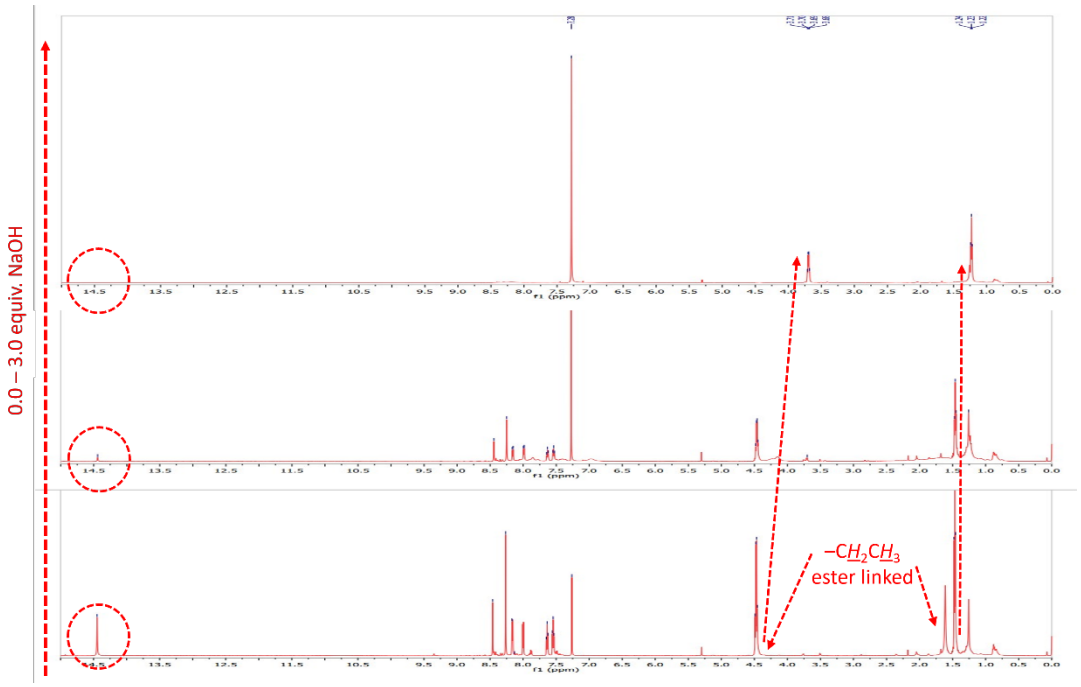

Fig. S25. ^{1}H NMR titration spectra for **L2** ($CDCl_3$) + NaOH (CD_3OD; 0.0 – 3.0 eq.).

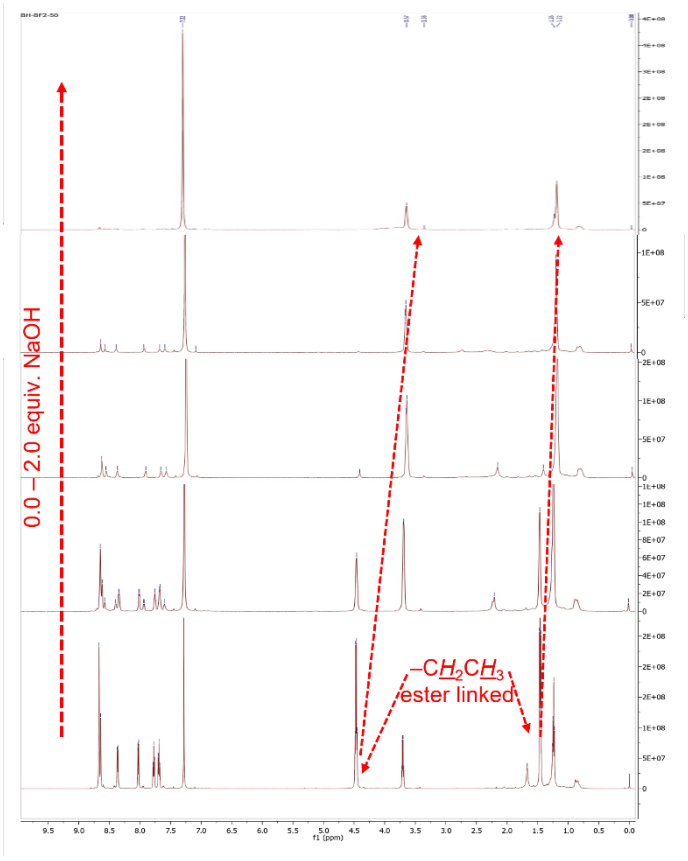

Fig. S26. ^{1}H NMR titration spectra for **B2** ($CDCl_3$) + NaOH (CD_3OD; 0.0 – 2.0 eq.).

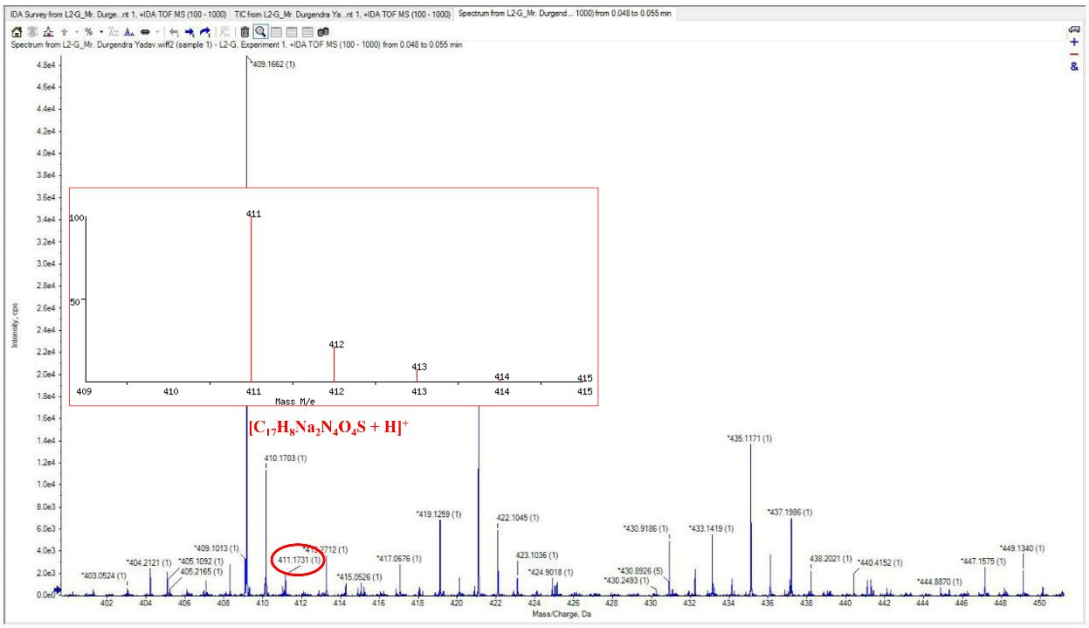

Fig. S27. Mass spectrum of **GL_2**.

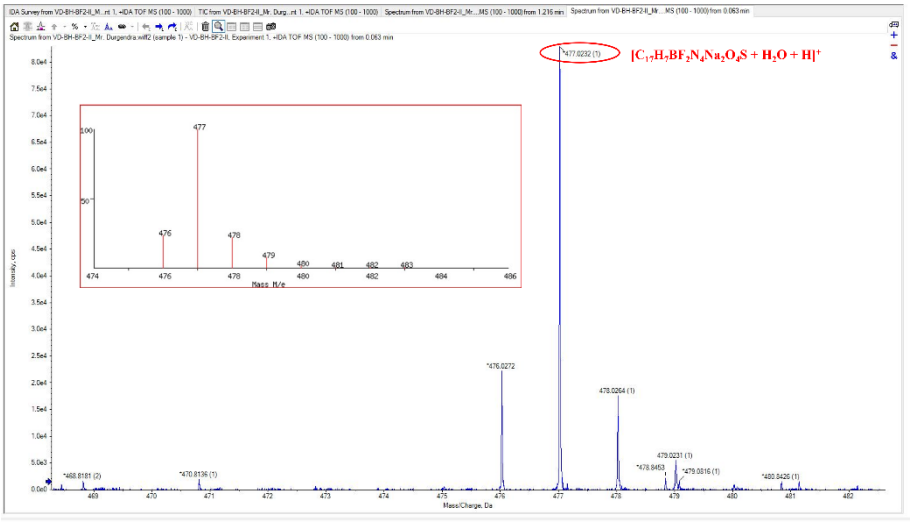

Fig. S28. Mass spectrum of **GB_2**.

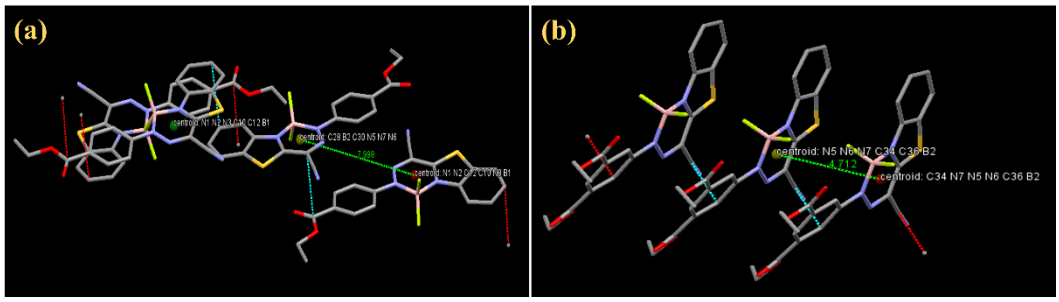

Fig. S29. Crystal packing of **B1** (a) and **B2** (b) showing potential π–stacking interaction between the subsequent molecular units (distance measured from centre of centroid).

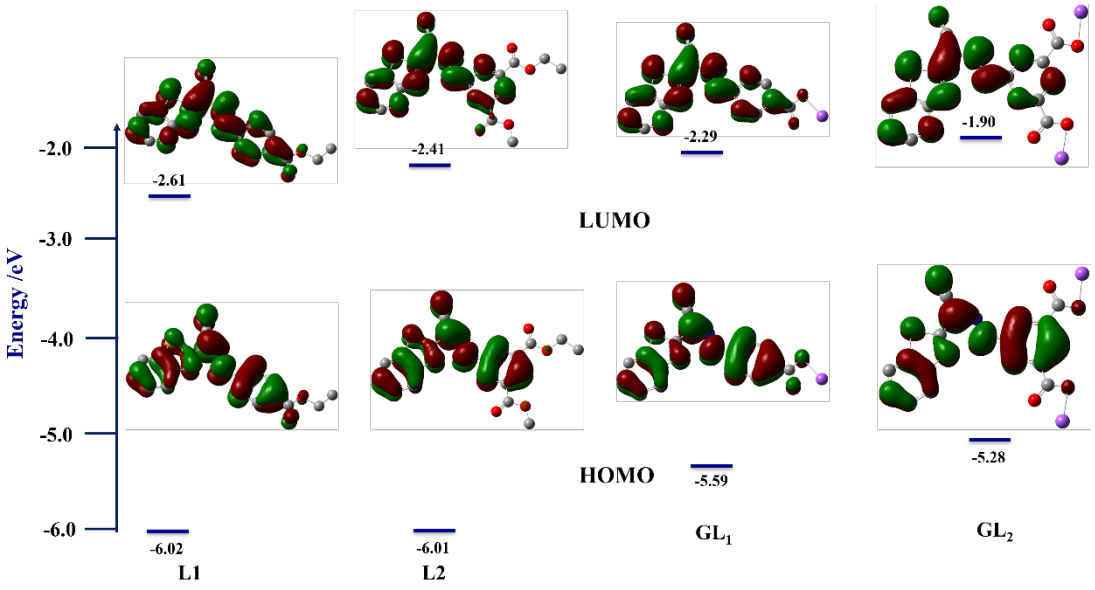

Fig. S30. DFT optimized structure of **L1**, **L2**, **GL_1** and **GL_2**.

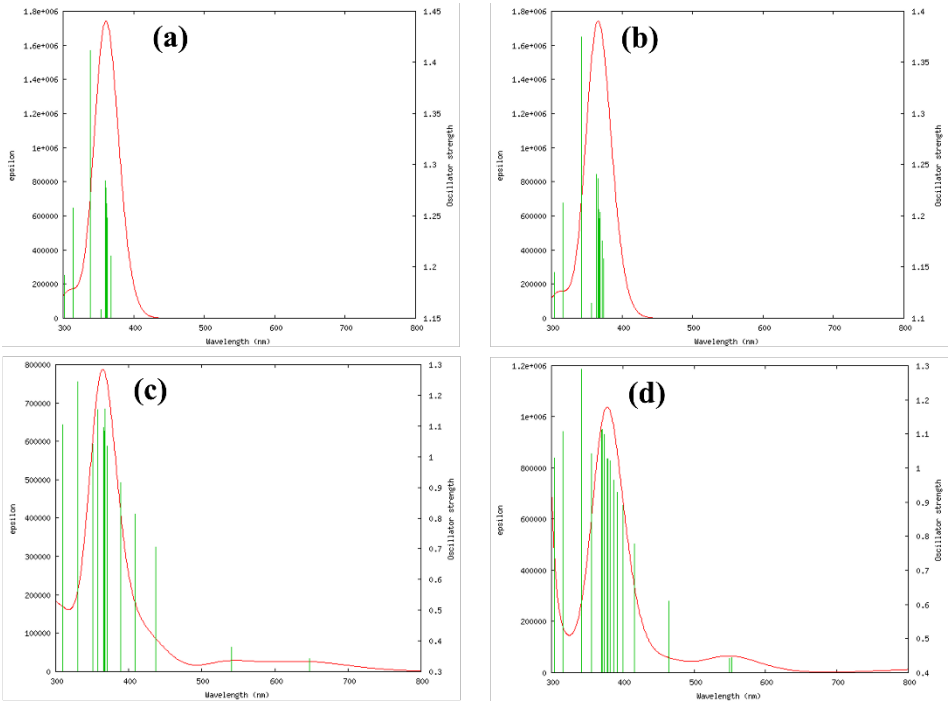

Fig. S31. UV–vis spectra of **L1** (a), **L2** (b), **GL$_1$** (c) and **GL$_2$** (d) obtained from TD–DFT calculations.

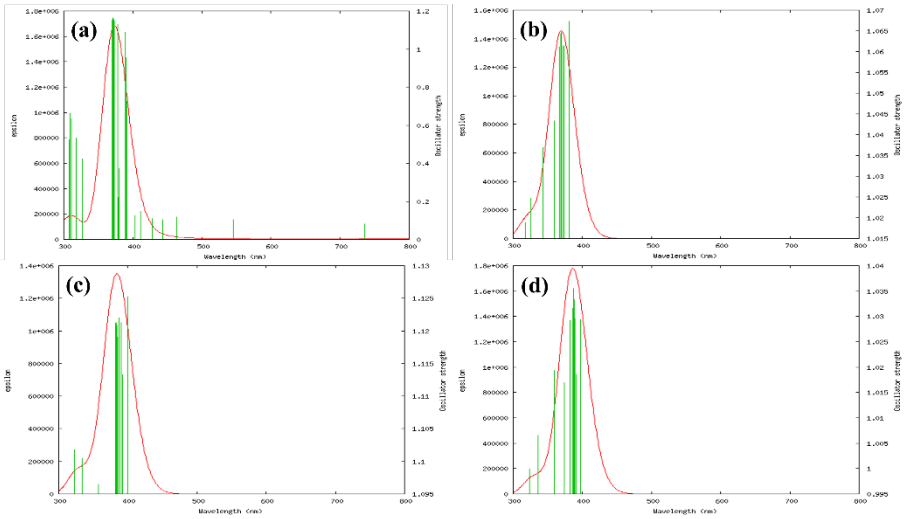

Fig. S32. UV–vis spectra of **B1** (a), **B2** (b), **GB$_1$** (c) and **GB$_2$** (d) obtained from TD–DFT calculations.

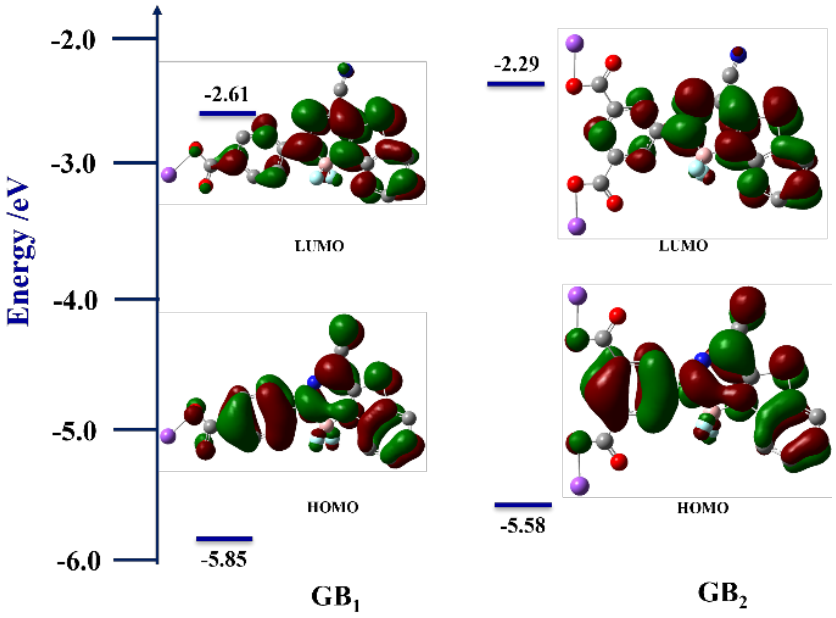

Fig. S33. DFT optimized structure of **GB$_1$** and **GB$_2$**.

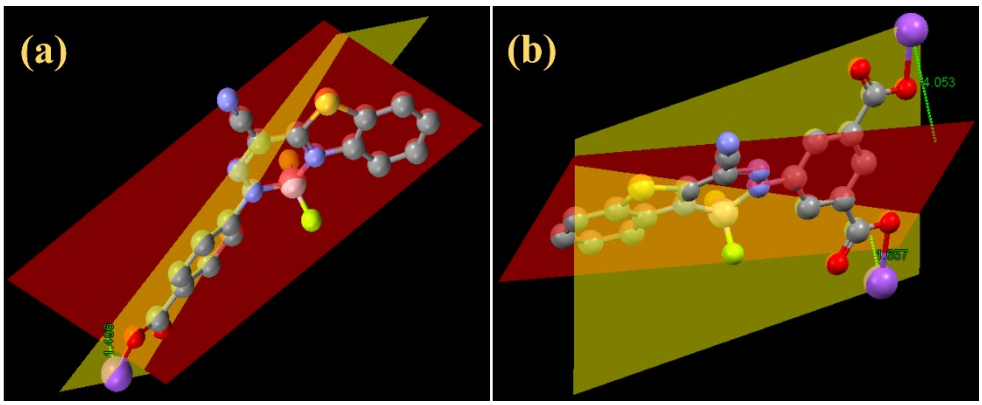

Fig. S34. Optimized structure of **GB$_1$** (a) and **GB$_2$** (b) (involvement and stabilization of Na^+ ion in BODIHYs).

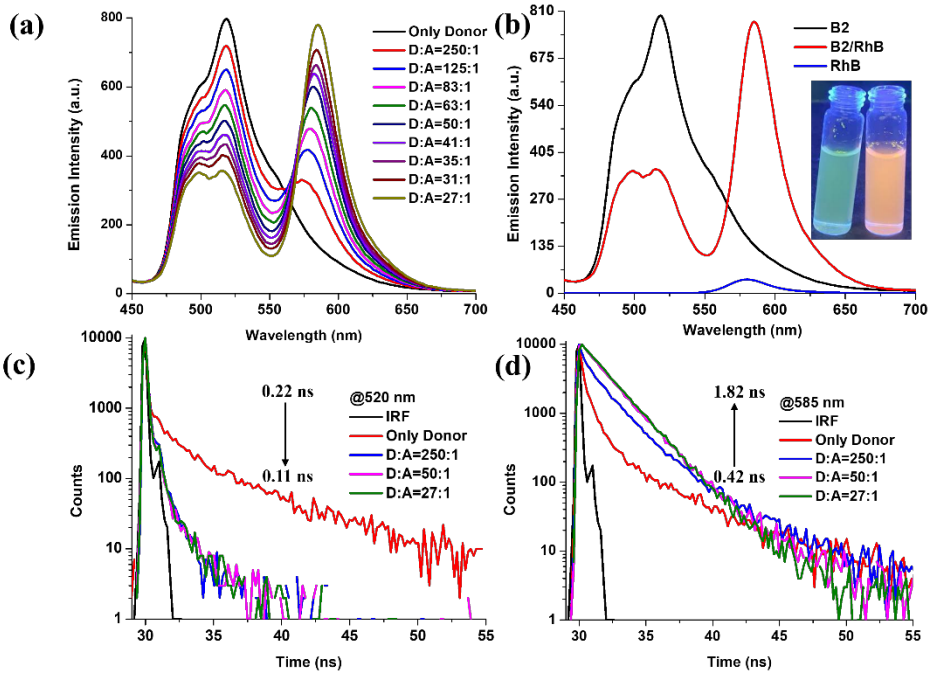

Fig. S35. (a) Fluorescence spectra of **B2** with gradual addition of RhB (λ_{ex} = 428 nm) in THF/water (f_w 90%) (c, 5.0 × 10^{-5} M and [RhB] c, 0.0, 0.2 × 10^{-6}, 0.4 × 10^{-6}, 0.6 × 10^{-6}, 0.8 × 10^{-6}, 1.0 × 10^{-6}, 1.2 × 10^{-6}, 1.4 × 10^{-6}, 1.6 × 10^{-6}, 1.8 × 10^{-6} M); (b) emission spectra of **B2** (50 μM), RhB+**B2** (c, 5.0 × 10^{-5} M, [RhB] c, 1.0 × 10^{-4} M) and RhB (c, 2.5 × 10^{-5} M); (c) and (d) Change in the fluorescence decay profiles of **B2** in the presence of RhB in THF/water (90%; v/v).

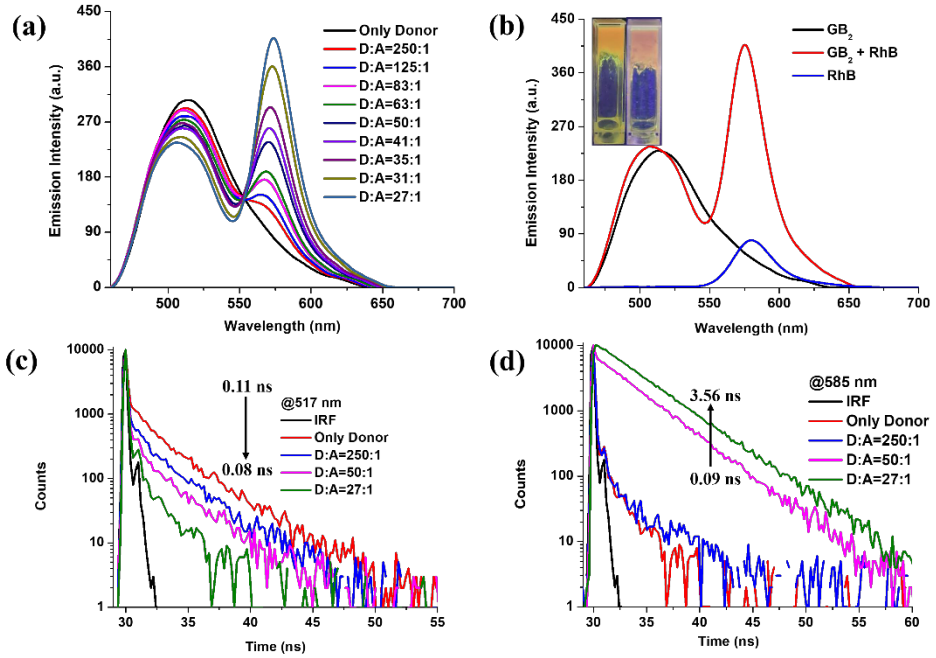

Fig. S36. (a) Fluorescence spectra of **GB_2** with gradual addition of RhB (λ_{ex} = 430 nm) in THF/water (f_w 90%) (*c*, 5.0 × 10^{-5} M and [RhB] *c* = 0.0, 0.2 × 10^{-6}, 0.4 × 10^{-6}, 0.6 × 10^{-6}, 0.8 × 10^{-6}, 1.0 × 10^{-6}, 1.2 × 10^{-6}, 1.4 × 10^{-6}, 1.6 × 10^{-6}, 1.8 × 10^{-6} M); (b) emission spectra of **GB_2** (50 μM), RhB+ **GB_2** (*c*, 5.0 × 10^{-5} M, [RhB], *c* = 1.0 × 10^{-4} M) and RhB (*c*, 2.5 × 10^{-5} M); (c) and (d) Change in the fluorescence decay profiles of **GB_2** in the presence of RhB in chloroform.

Table S1: Crystal Data and Structure Refinement Parameters for L1, L2, B1 and B2.

Crystal parameters	L1	L2	B1	B2
Empirical formula	$C_{18}H_{14}N_4O_2S$	$C_{21}H_{18}N_4O_4S$	$C_{18}H_{13}BF_2N_4O_2S$	$C_{21}H_{17}BF_2N_4O_4S$
Formula weight	350.08	422.10	398.19	470.26
Crystal system	Monoclinic	Triclinic	Monoclinic	Monoclinic
Space group	P 1 21/c 1	P – 1	P 1 21/n 1	P 1 21/c 1
a (Å)	18.7707(6)	6.1374(1)	7.0123(3)	25.7435(3)
b (Å)	4.4024(1)	9.8205(2)	19.0989(6)	4.7116(1)
c (Å)	22.1747(7)	17.4591(4)	27.0005(8)	36.3900(4)
α (deg)	90.00	105.187(2)	90.00	90.00
β (deg)	114.284(4)	91.749(2)	92.285(3)	95.568(1)
γ (deg)	90.00	94.127(2)	90.00	90.00
V ($Å^3$)	1670.29(10)	1011.58(4)	3613.2(2)	4393.0(12)
Color and habit	Yellow, needle	Brown, needle	Yellow, needle	Red, needle
Z	47	4	41	41
dcal (g/cm^3)	1.393	1.387	1.464	1.422
Temperature (K)	293	293	293(2)	293(2)
wavelength (Å)	1.54184	1.54184	1.54184	1.54184
μ (mm^{-1})	1.891	1.735	1.978	1.787
GOF on F^2	1.0295	1.140	1.039	1.039
R indices (All data)	R_1 = 0.0857 wR_2 = 0.1248	R_1 = 0.1063 wR_2 = 0.2972	R_1 = 0.0926 wR_2 = 0.2352	R_1 = 0.0602 wR_2 =0.1418
final R indices [I > 2σ(I)]	R_1 = 0.0450 wR_2 = 0.1037	R_1 = 0.0957 wR_2 = 0.2869	R_1 = 0.0788 wR_2 = 0.2289	R_1 = 0.0445 wR_2 =0.1257

Table S2. Selected crystallographic parameter for B1

B1	Bond Length (Å)	B1	Bond Angle (º)
S1–C12	1.714(5)	**C18–S1–C12**	89.6(3)
S1–C18	1.739(6)	**C3–O1–C2**	118.5(4)
F1–B1	1.375(9)	**C7–N1–N2**	113.6(4)
F2–B1	1.355(9)	**B1–N1–N2**	126.5(4)
O1–C2	1.445(6)	**B1–N1–C7**	124.3(5)
O1–C3	1.328(7)	**O2–C3–O1**	123.6(5)
O2–C3	1.198(7)	**F2–B1–F1**	111.8(6)
N4–C11	1.139(8)	**N1–B1–F1**	110.3(6)
N1–B1	1.572(8)	**N1–B1–F2**	110.5(5)
N3–B1	1.562(7)	**N3–B1–F1**	107.7(5)
N1–N2	1.317(6)	**N3–B1–F2**	109.6(6)
		N3–B1–N1	106.6(5)

Table S3. Selected crystallographic parameter for B2

B2	Bond Length (Å)	B2	Bond Angle (º)
S1–C15	1.7147(18)	**C15–S1–C16**	89.84(9)
S1–C16	1.7456(19)	**N2–N1–B1**	126.35(14)
F1–B1	1.372(2)	**O3–C10–O4**	123.1(2)
F2–B1	1.373(2)	**O2–C3–O1**	123.6(2)
N3–B1	1.559(2)	**F2–B1-N3**	109.55(15)
O1–C3	1.316(3)	**F2–B1–N1**	110.67(15)
O2–C3	1.192(3)	**F1–B1–F2**	111.11(15)
O3–C10	1.194(3)	**F1–B1–N3**	109.22(15)
O4–C10	1.329(3)	**F1–B1–N1**	109.78(14)
		N3–B1–N1	106.39(13)
		N3–C15–S1	114.54(13)
		N3–C15–C13	120.28(16)

Table S4. Some important short interactions in **B1** and **B2**.

Short interactions in B1	**Distance (Å)**	**Short interactions in B2**	**Distance (Å)**
C–H···H–C	2.392	**N···H**	2.633, 2.696
O···H	2.362	**F···H**	2.651, 2.610
S···H	2.976	**S···N**	2.886
π···O	3.126	**π···H**	2.886
S···O	2.985	**O···H**	2.596, 2.599
		π···F	2.929, 2.930

Table S5. Gelation behaviour of **L1**–**L2** and **B1**–**B2**.

Sr. No.	**Solvents**	**Solubility of L1 and L2**	**State on addition of NaOH solution**	**Solubility of B1 and B2**	**State on addition of NaOH solution**
1	**$CHCl_3$**	Soluble	Suspension – **L1** Gel – **L2**	Soluble	Suspension – **B1** Gel – **B2**
2	**CH_2Cl_2**	Soluble	Suspension	Soluble	Suspension
3	**CH_3CN**	Soluble	---	Soluble	---
4	**THF**	Soluble	---	Soluble	---
5	**1,4–dioxane**	Soluble	---	Sparingly soluble	---
6	**CH_3COCH_3**	Soluble	Suspension	Soluble	Suspension
7	**DMF**	Soluble	Sol	Soluble	---
8	**DMSO**	Soluble	Sol	Soluble	Sol
9	**Ethyl Acetate**	Soluble	Suspension	Soluble	---
10	**CH_3OH**	Soluble	---	Less Soluble	---
11	**C_2H_5OH**	Less Soluble	---	Less Soluble	---
12	**Hexane**	Insoluble	---	Insoluble	---
13	**C_6H_6**	Insoluble	---	Less soluble	---

Table S6. Experimental/theoretical absorption wavelength, energy, oscillation strength (*f*) and assignments

	Experimental Wavelength (nm)	**Calculated Wavelength (nm)**	**Oscillator Strength (*f*)**	**Energy (eV)**	**% Contribution**	**Assignments**
L1	403	363	1.236	3.41	88	H → L
L2	392	358	1.13	3.52	85	H → L
B1	428	391	0.7242	3.28	87; 4; 4	H → L; H–8 → L, H–4 → L
B2	421	370	1.06	3.41	88; 4	H → L; H–4 → L

References

1. D. D. Perrin, W. L. F. Armango and D. R. Perrin, Purification of Laboratory Chemicals, Pergamon, Oxford, U. K., 1986.
2. Sheldrick GM. SHELXL–97, Program for X-ray Crystal Structure Refinement, Gottingen University, Gottingen, Germany, 1997.
3. Sheldrick GM. SHELXS–97, Program for X-ray Crystal Structure Solution, Gottingen University, Gottingen, Germany, 1997;
4. Sheldrick GM. Crystal structure refinement with SHELXL Acta Crystallogr., Sect. C: *Struct. Chem*, 2015, **71**, 3–8.
5. R. Ditcrfield, W. J. Herre, and J. A. Pople, *J. Chem. Phys.*, 1971, **54**, 724–729.
6. W. Kohn and L. Sham, *Phys. Rev.*, 1965, **140**, 1133–1138.
7. A. D. Becke, *J. Chem. Phys.*, 1992, **97**, 9173–9178.
8. A. Kumar, R. S. Singh, A. Kumar, A. Ali, A. Biswas, and D. S. Pandey, *Chem. Eur. J.*, 2016, **22**, 13799–13804.